Timing of readiness potentials reflect a decision-making process in the human brain

Kitty K. Lui[1], Michael D. Nunez[2,1], Jessica M. Cassidy[3], Joachim Vandekerckhove[1,4], Steven C. Cramer[3,5], Ramesh Srinivasan[1,2,*]

[1]Department of Cognitive Sciences, University of California, Irvine USA
[2]Department of Biomedical Engineering, University of California, Irvine USA
[3]Department of Neurology, University of California, Irvine USA
[4]Department of Statistics, University of California, Irvine USA
[5]Department of Anatomy & Neurobiology, University of California, Irvine USA
[*]Corresponding Author

Abstract

Perceptual decision making has several underlying components including stimulus encoding, perceptual categorization, response selection, and response execution. Evidence accumulation is believed to be the underlying mechanism of decision-making and plays a decisive role in determining response time. Previous studies in animals and humans have shown parietal cortex activity that exhibits characteristics of evidence accumulation in tasks requiring difficult perceptual categorization to reach a decision. In this study, we made use of a task where the challenge for the participants is to identify the stimulus and then from memory apply an abstract rule to select one of two possible actions. The task was designed so that stimulus identification was easy but response selection required cognitive computations and working memory. In simultaneous EEG recordings, we find a *one-to-one* relationship between the duration of the *readiness potential* observed prior to the response over motor areas, and *decision-making time* estimated by a drift-diffusion model of the response time distribution. This close relationship implies that the readiness potential reflects an evidence accumulation process for response selection, and supports the notion that evidence accumulation is a general neural implementation of decision-making. The evidence accumulation process that captures variability in decision-making time will depend on the location of the bottleneck in information processing.

Introduction

Decision-making has been extensively studied using two-alternative forced choice tasks that incorporate multiple stages of information processing (Ratcliff et al., 2016). In these tasks, participants typically perceive a visual or auditory stimulus (perception), evaluate and assign it one of two categories (decision-making), and respond with one of two responses (response selection and execution). Behavioral data consisting of response time and accuracy have been modeled by a number of sequential-sampling models (SSM) that incorporate perceptual evidence sampling such as the drift-diffusion model (Link & Heath, 1975; Ratcliff & McKoon, 2008), linear ballistic accumulator model (Brown & Heathcote, 2008) or leaky competing accumulator model (Usher & McClelland, 2001). At the heart of all of these models is the notion that decision-making can be modeled as accumulating evidence to a boundary or criterion level which triggers the motor response. These models typically assume that each of the many underlying cognitive operations is a separate step and performed in sequence. For example, in a simple drift-diffusion model, one might assume that response time can be decomposed into three sequential time periods, 1) time for perceptual processing, 2) time for accumulation of evidence, modeled by a random walk, and 3) time for response selection and execution. In this study we show that the readiness potentials (RP) recorded over motor areas of the brain initiates prior to decision-making and has duration that tracks decision-making time. This challenges the assumption by the SSMs of a period of perceptual evidence accumulation followed by a *sequential* period of response processing, and instead indicates that the motor system engages in a parallel evidence accumulation process to reach an action decision.

Direct recordings from parietal cortical neurons in monkeys have identified cells whose firing rates progressively increase prior to a decision and response (Roitman and Shadlen, 2002; Huk and Shadlen, 2005, Churchland et al., 2008). The changing firing rates of these neurons are consistent with the theoretical account of accumulation of evidence to a boundary that is central to decision-making SSMs. Moreover, in these studies, as the strength of sensory signals increases the rate of increase in firing rate is enhanced, suggesting a faster rate of information accumulation that leads to faster response times (Roitman & Shadlen, 2002). Similar results have been found in the motor system, specifically in the frontal eye fields (FEF), where cells related to control of eye movements exhibit faster rate of growth of firing rate as speed increases, i.e., response time decreases (Kim & Shadlen, 1999). These results all point to the idea that the ramping of firing rates is a generic neural implementation of evidence accumulation leading to a decision (Shadlen & Kiani, 2013).

These findings in animal models have motivated studies in humans using EEG to identify a signal that ramps to a decision threshold, providing independent information about the rate and timing of decision making (Kelly & O'Connell, 2013; Philiastides, 2014). The typical response

times in perceptual decision-making tasks, estimated evidence accumulation rates (drift rates), and the observed firing-rate ramps in animal models suggest slow neural processes on the order of 100s of ms, typical of slow oscillations in EEG. A number of studies have focused on the P300, a stimulus-locked evoked potential that increases its positive amplitude over parietal electrodes reaching a maximum at least 300 ms after stimulus presentation (Philastides et al., 2006; Ratcliff et al., 2009; O'Connell et al., 2012; Kelly & O'Connell, 2013). This signal has also been labeled central-parietal positivity (CPP) to better account for the variability in the timing of the peak of the positive potential across different experiments. The P300/CPP amplitude is sensitive to stimulus probability and stimulus salience (Smith & Ratcliff, 2004; Polich et al., 1996), such that low-probability and high-salience sensory events elicit higher amplitude signals. Moreover, the parietal P300/CPP has been observed for both auditory and visual stimuli, indicating that it is supramodal (O'Connell et al., 2012; Polich et al., 1996).

Both the amplitude and the timing of the CPP/P300 have been suggested as indicators of the evidence accumulation process. In a study using stimuli with different levels of salience and a categorical discrimination (face/car), the magnitude of this parietal signal correlated to the drift-rate in a drift-diffusion model of the response data (Philiastides et al., 2006). In another study using vigilance tasks, the detection of gradual reductions in stimulus contrast evoked a CPP/P300 that was delayed as response time increased and peaked at the time of response execution (O'Connell et al., 2012). Critically, this signal was found across sensory modalities (auditory and visual) and even in tasks not requiring a motor response. A similar effect could be observed for motion discrimination, with a delayed and smaller CPP/P300 peak as motion coherence decreased (Kelly & O'Connell, 2013). However, because of the gradual changes of the stimuli in these vigilance tasks, at least some of these effects might be accounted for by the delay in detection of the onset of the target stimuli, which is reflected in a delayed onset of the CPP/P300 and hence a delayed peak. Implicit in the design of these experiments is the notion that the action, or motor output, follows immediately from the recognition of the stimulus. Thus the decision-making challenge in these tasks is only in the perceptual categorization due to varying stimulus signal-to-noise ratios. The tasks have no additional load on working memory or on cognitive computations, such as the application of an abstract rule to make a decision.

In the current study, we make use of a two-alternative forced choice task labeled the action selection (AS) task (O'Shea et al., 2007). The AS task makes use of simple visual stimuli presented with no noise. Decision-making requires the subjects to remember an abstract rule about the visual stimulus that encodes the stimulus-response mapping and to execute as rapidly as possible accordingly to the rule (O'Shea et al., 2007). For comparisons, we also made use of an execute only (EO) task to potentially separate decision-making from motor execution. The EO task is a simple response time task, requiring subjects to react and execute the same motor movement as fast as possible when cued by any visual stimulus (O'Shea et al., 2007).

The critical stages of decision-making in the AS task take place after recognition of the stimulus, potentially in neural systems responsible for response selection. The Bereitschaftspotential (BP) or readiness potential is an EEG slow wave potential recorded over the midline close to motor areas that ramps as early as two secs prior to a self-generated movement and reaches a negative peak at movement onset (Kornhuber & Deecke, 1964; Shibaski & Hallet, 2006). BP can be characterized into two components, early BP and late BP (also called Negative Slope), and is specific to self-paced movements. Early BP is prominent over midline areas, like supplementary motor areas (SMA) and pre-SMA, with a shallow negative slope. In late BP, there is a steeper negative slope over contralateral motor areas that starts around 400-500 ms before movement. Similar slow-wave potentials are also observed for stimulus-cued movements (Shibaski & Hallet, 2006). Since BP is a specific term for self-paced movements and the current paper employs externally cued movements, we label the slow wave potential preceding cued movements as the readiness potential (RP). The RP exhibits spatial and temporal characteristics similar to the BP and has been interpreted as the activation of motor areas in preparation for response-selection (Eimer, 1998). Choice tasks that do not require a motor response also elicit the RP, suggesting that the RP is related to decision-making (Alexander et al., 2016), consistent with a role in response selection rather than response execution.

In this paper, we use a drift-diffusion model to separate the contributions of *non-decision time* (for perceptual processing and motor execution) and *decision-making time* to response time while subjects perform the Action Selection (AS) task. In the AS task, an abstract rule must be applied to the stimulus to accumulate evidence to select one *action* over the other. We find that the onset of the readiness potential (RP) immediately follows visual encoding and is invariant of task or response time and that the duration of the RP has a one-to-one relationship with decision-making time, i.e., the time duration of evidence accumulation.

Methods

Participants

Fifteen adults (age 18-26 years; 10 females) participated in this study. All subjects met the following inclusion criteria: at least 18 years of age, right-handed, and English-speaking. Right hand dominance was verified using the Edinburgh Handedness Inventory (Oldfield, 1971). Subjects were not able to participate if they demonstrated any of the following exclusionary criteria: inability to maintain attention or understand verbal instructions, any major neurological, psychiatric, or medical disease, or a coexisting diagnosis impacting arm/hand function.This study was approved by the University of California, Irvine Institutional Review Board. Each subject provided written informed consent.

Procedure

Participants performed two different tasks requiring evaluation of a visual stimulus and a motor response. Each sat with back on a chair, hips and knees at approximately 90 deg, and right forearm in a splint. Subjects completed 4 blocks (40 trials per block) of the AS task and 4 blocks (40 trials per block) of the EO task. The blocks alternated for all subjects, starting with AS task. Each block of trials began with an instruction presented for 30 seconds (Figure 1A). On each trial (Figure 1B), subjects focused on a fixation cross. A stimulus (i.e., shape) appeared for two seconds and the response was given by the internal (inward) or external (outward) rotation of the right shoulder by 17.5 degrees using a forearm splint apparatus (Figure 1C), until the splint made contact with a button embedded in either lateral wall. The purpose of the splint apparatus was to minimize compensatory movements by forearm and/or hand and thereby limit movement to a single direction in a single joint, i.e., right shoulder rotation. Subjects responses were recorded when they depressed the button, indicating movement completion. Subjects received verbal instruction to go back towards the middle of the splint after each trial. The interstimulus interval was randomized between 1 to 3.5 seconds. After each block, subjects received a 30-second rest break that was prompted by a black screen on the laptop (Figure 1B).

Experimental Tasks

The Action Selection (AS) task (O'Shea et al., 2007) is a two-alternative forced choice (2AFC) task. Participants were instructed to perform external right shoulder rotation (move the splint outward) when they saw either a big square or small circle, and instructed to perform internal right shoulder rotation (move the splint inward) when they saw either a big circle or small square. The large shapes spanned 2 degrees of visual angle while the small shapes spanned 1 degree of visual angle.

The Execution Only (EO) task is a simple reaction time task. Participants were instructed to move their right forearm, via shoulder rotation, to only one side within a given block, upon stimulus onset, irrespective of the size and shape presented. The EO blocks alternated between performing only internal rotations and performing only external rotations.

Drift-Diffusion Parameter Estimation

The behavioral data (i.e., response time and choice data) were analyzed with an hierarchical drift-diffusion model, using a Bayesian estimation method with Markov Chain Monte Carlo samplers (Plummer, 2003; Lee & Wagenmakers, 2014; Vandekerckhove et al., 2011; Waberisch

and Vandekerckhove, 2014). Fitting parameters of drift-diffusion models adds to the analysis of human behavior by assuming simple underlying cognitive processes which have some empirical validation (Voss et al., 2004). Drift-diffusion models also add to the cognitive interpretation of EEG and functional magnetic resonance imaging (fMRI) signals by relating cognitive parameters to observed cortical dynamics (Mulder et al., 2014; Turner et al., 2015; Turner et al., 2017; Nunez et al., 2015, 2017). In a drift-diffusion model it is assumed that humans accumulate evidence for one choice over another in a random-walk evidence-accumulation process with an infinitesimal time step until sufficient evidence is accumulated to exceed the threshold for either the correct or the incorrect choice option. That is, evidence E accumulates following a Wiener process (i.e. Brownian motion) with a drift rate $\boldsymbol{\delta}$ and diffusion coefficient or instantaneous variance $\boldsymbol{\varsigma^2}$ (Ross, 2014) until enough evidence $\boldsymbol{\alpha}$ for a correct decision over an incorrect decision is made (see Ratcliff & McKoon, 2008 for a further discussion). The instantaneous variance parameter was set to 1.0 in this study, because only two of the three evidence dimension parameters can be estimated without additional data (Ratcliff, 1978; Nunez et al., 2017).

Response time is defined as the amount of time after the stimulus onset for the subject to depress one of the two lateral wall buttons with the forearm splint apparatus. *Decision-making time* is the amount of time it takes to accumulate evidence to threshold (e.g. via the random walk process), while *non-decision time* is the amount of time not associated with evidence accumulation, such as *visual encoding time* (i.e. the amount of time that the brain takes to recognize that evidence must be accumulated after visual onset) and *motor execution time* (i.e. any time after decision making occurs but before the response is recorded by the computer, including arm movement time in the apparatus).

Our theoretical model also assumed that all participants had different perceptual decision-making neural processing speeds. Each cognitive parameter of each participant was drawn from a single task-level population (AS or EO). This meant that we assumed that drift-diffusion cognitive parameters (drift rate, boundary separation, and non-decision time) varied across participants and the two tasks, but that there was similarity across the participants in each task. Adding these *hierarchical* parameters yields better estimates of parameters due to *shrinkage*, a phenomenon whereby parameters are better estimated because hierarchical relationships enforce similarity across each parameter. Condition-level Bayesian priors for hierarchical drift-diffusion model parameters were wide normal distributions. The prior distributions were centered at 1 for drift rate $\boldsymbol{\delta}$ and decision-evidence required $\boldsymbol{\alpha}$ with 2 and .5 standard deviations (in arbitrary evidence units dependent upon the scale of instantaneous variance). The prior distribution for non-decision time $\boldsymbol{\tau}$ was centered at 300 ms with a standard deviation of 250 ms and truncated at 0 ms.

For this study, only posterior distributions of non-decision time $\boldsymbol{\tau}$ for the two tasks were analyzed because our hypotheses involved only the decision time and non-decision time per subject and

not the underlying shape of decision and non-decision time distributions. Medians of posterior distributions of non-decision time were used as estimates of the most-likely values for those parameters and were subtracted from response times on each trial to obtain estimates of decision-making time for each trial.

EEG Recording

The subjects were fit with a 256-electrode EEG cap (HydroCel Sensor Net, Electrical Geodesics, Inc., Eugene, Oregon, USA). The cap was placed on the participant's head after 10 practice trials of the AS task were completed to familiarize them with the experimental procedures. EEG data were sampled at 1000 Hz using a high-input impedance Net Amp 300 amplifier (Electrical Geodesics, Inc.) and NetStation 4.5.3 software. The EEG signals were referenced to the vertex electrode (Cz) during recording. The inputs from the splint apparatus were recorded by the EEG amplifier, using separate channels to record respective buttons for internal and external rotations shoulder rotation movements. The onset of the stimulus was recorded by the EEG amplifier using a light detector (Cedrus, San Pedro, California, USA) for precise timing information synchronized with the EEG.

EEG Preprocessing

All EEG analysis was performed using original MATLAB (Natick, MA) programs. The EEG data were segmented into trials starting 1000 ms prior to stimulus onset up to 2500 ms after the stimulus for a total duration of 3500 ms. Any trials where the participants either responded incorrectly (wrong rotation direction), did not respond at all, or responded either too rapidly (within 200 ms) or too slowly (more than 2.3 seconds) from the stimulus onset, was deemed an incorrect response. If participants responded more than once in one trial, the first response was considered their response. Bidirectional autoregressive interpolation was performed on each EEG channel from 5 to 30 samples after the response on each trial to remove an artifact created in the EEG by the input signal from the switches on the splint apparatus. As all data analysis took place in the interval prior to the response, this interpolation did not affect any of the results and was only performed to facilitate visualizing the results.

Each trial was detrended to remove any linear trends. Butterworth filters to high-pass filter at 0.25 Hz (0.25 Hz pass, 0.1 Hz stop, 10 dB loss) and notch filter at 60 Hz (pass below 59 Hz and above 61 Hz, 10 dB loss) was applied to the data. The process of cleaning EEG data removed some stereotypical artifacts generated from events such as eye movement, jaw movements, or muscle activity (Nunez et al., 2016). By visual inspection, trials that contained any vigorous movement and channels frequently containing EMG artifacts were removed from further data analysis. After the manual inspection, the data were re-referenced to the common-average

reference. Independent Component Analysis (ICA) was then used to classify and remove artifacts from data that were related to eye movements and electrodes that picked up environmental noise. ICA components were assessed as clearly artifact or possibly containing EEG (Nunez et al., 2016). For the purpose of this data analysis, all components not marked as artifact were kept for data analysis, and only components that clearly captured artifacts such as eye blinks, eye movements, or isolated channel pops were removed. The ICA components were then projected back into channels and the data were low-pass filtered at 50 Hz (Butterworth filter, 50 Hz pass, 60 Hz stop, 10 dB loss).

Evoked potentials

For each subject, *stimulus-locked* evoked potentials (EPs) were calculated at each channel by aligning each trial to the marker of the stimulus onset and averaging across trials and *response-locked* evoked potentials were calculated by aligning to the marker of the button depression and averaging across trials. We refer to the response-locked evoked potentials as readiness potentials (RPs). As our focus in this paper was on slow-wave potentials, the evoked potentials were low-pass filtered at 4Hz (Butterworth filter, 4 Hz pass, 8 Hz stop, 10 dB loss). In preliminary analyses, only a trivial difference was found in either stimulus-locked EPs or response-locked RPs between internal and external shoulder rotations in the low-pass filtered signals. Thus, we analyzed the data combining trials for the two directions of rotation to compute the evoked potentials. For the stimulus-locked EPs, results are presented from 400 ms before the stimulus to 1500 ms after the stimulus, and baseline correction was performed by subtracting the mean potential 400 to 200 ms before the stimulus onset. For the response-locked RPs, the results are presented from 1200 ms before the response to 100 ms after the response, with baseline correction performed by subtracting the mean potential in the interval 1200 to 1000 ms before the response.

Evoked Potentials with Response Time Tertile Split

The response times for each subject were divided into three equal-sized bins to separate them into different response speed conditions (i.e., fastest, middle, slowest). The stimulus-locked EPs and response-locked RPs were calculated separately by averaging trials within the three tertiles. For the RPs, the time interval analyzed for the fastest and middle conditions were 1200 ms before the response and 100ms after the response as in the overall average. A different time interval had to be chosen for the slowest condition in order to accurately estimate the onset time due to trials with response times longer than 1000 ms. The time interval analyzed was 1400 ms before the response and 100 ms after the response, and baseline correction was performed by subtracting the mean potential in the interval 1400 to 1200 ms before the response. The fastest

and middle RT trials could not have had an extended window like the slowest condition as they would potentially overlap with data from the previous trial.

Timing of the Readiness Potential: RP duration and RP onset time

We characterized the timing of the readiness potential (RP) in terms of duration and onset time following stimulus presentation. The readiness potential is calculated by averaging the EEG data aligned to the response. We identified the 8 channels (out of 256) that displayed the strongest negative potential prior to the motor response which is the defining characteristic of readiness potentials. These 8 channels were located close to the midline and slightly left-lateralized over motor areas of the brain (see Figure 3). RP duration was defined as the interval during which the potential remains consistently negative at these channels, starting from the initial negative deflection up to the response execution. To identify this interval, the first derivative of the RP was estimated by taking the difference of the potential at each time point from the previous time point. The start of the readiness potential was detected at the center of the first interval where the derivative remains negative for 125 ms indicating a consistent negative deflection of the evoked potential. The duration of the RP was defined as interval from this starting point to the button press. The onset time of the readiness potential relative to stimulus presentation was calculated from the stimulus-locked EPs at the same 8 channels with the requirement that derivative must have remained negative for 100 ms to locate the onset of the negative deflection.

Statistical Tests

Analysis with linear models was performed on response-locked RP durations, stimulus-locked EP onset times, and response time (RT) distribution statistics. Mixed-effects ANOVA models were used to assess the effect of task with subjects as a random factor. In the RT tertile analysis, task and RT tertile were fixed factors, while subjects were a random factor. Statistics reported are both F statistics and associated p-values as well as the Bayes Factors (BF) which describe the amount of evidence for a model with different means relative to a model with only one mean for both tasks, or for RT tertiles (Rouder et al., 2012).

Linear regression models between RP duration and response time or decision time with were also carried out and a conventional F-statistic on the model is presented. The amount of evidence for a model that has a non-zero regression slope over a model which has a regression slope of zero (Kass and Raftery, 1995; Rouder and Morey, 2012) is presented as a Bayes Factor (*BF*). Adjusted R^2 is also reported and describes the fraction of variance of the dependent variable (e.g. response time median) explained by the regressor variable (timing measures of RP). Bayes Factors (*BF1*) comparing models with regression slopes equal to 1, indicating a 1-to-1 relationship, to models with unknown regression slopes were calculated by first fitting simple

regression models in JAGS (Plummer, 2003) with wide priors on slope parameters (normal distribution centered on 1 with a standard deviation of 3) and then using the simple Savage-Dickey Density Ratio (Dickey and Lientz, 1970; Wagenmakers et al., 2010). All other statistics were generated by either JASP, an open-source graphical software package for statistical analysis (JASP Team, 2017), or MATLAB (Natick, MA).

Surface Laplacian

The surface Laplacian was applied to the RPs to improve spatial resolution of the EEG. The surface Laplacian is the second spatial derivative of the EEG along the scalp surface, and provides an estimate of the location of focal superficial cortical sources (Nunez and Srinivasan, 2006). The scalp surface was modeled using the MNI-152 average head (Mazziota et al., 1995), and the surface Laplacian was calculated along a triangular mesh representing the scalp using a three-dimensional spline algorithm (Deng et al., 2012).

Results

Behavioral Data: Response Time and Accuracy

Response times for the Action Selection (AS) task ($\bar{x}$ = 1041 ms, *Md* = 1090 ms, *s* = 139 ms) were much longer than the Execution Only (EO) task ($\bar{x}$ = 632 ms, *Md* = 638 ms, *s* = 111 ms). A mixed-effects ANOVA model was used to analyze the response times to estimate the effect of task and direction of rotation with participants treated as a random factor. There was a significant effect of task on response time; $F(1,14) = 353.53$, $p < .001$, with a decisive Bayes Factor ($BF = 10^{19}$) supporting longer response times in the AS task. There was an undetermined effect of rotation; $F(1,14) = 27.88$, $p < .01$, with $BF = 0.75$. Accuracy was very high for both the EO task ($\bar{x}$ = .99, *s* = .003) and the AS task ($\bar{x}$ = .97, *s* = .03). As a consequence, we performed EEG analysis using all the trials.

Drift Diffusion Model: Decision and Non-Decision Time

We modeled the response time distributions with the drift-diffusion model to separate non-decision time for perceptual processing and motor execution from decision-making time. The response time distribution for each subject is shown for each task in Figure 2. The EO task was performed faster and with less variability across trials in each subject (Figure 2, red histograms) compared to the AS task (Figure 2, blue histograms). This result was expected since the EO task does not require time to recall the mapping between stimuli and responses and assess which response correctly follows the stimulus. Posterior distributions of the non-decision time parameter were estimated for both tasks across subjects (population level in the hierarchical

model) and for each subject in each task. For each subject and task a 95% credible interval of the non-decision time is presented by a shaded bar in Figure 2. The fastest response times in each tasks are good approximations of each participant's non-decision time. There is a wide variability in non-decision times across participants but a relatively narrow 95% credible interval within each subjects data.

For the AS task, the median of the population-level posterior distribution of non-decision time was 464 ms with a 95% credible interval ranging from 421 ms to 508 ms. For the EO task, the median of the population-level posterior distribution of non-decision time was 292 ms with a 95% credible interval ranging from 247 ms to 335 ms. There was no overlap found between the distributions for the two tasks indicating that the probability of the non-decision times being the same between the AS task and the EO task was essentially zero.

Response time is composed of decision-making time and non-decision time. For the AS task, median response time was 1090 ms, and non-decision time median was 464 ms, indicating typical decision-making time of around 630 ms. In the EO task, median response time was 638 ms, and non-decision time median at 292 ms, indicating typical decision time of approximately 345 ms. Thus, the longer response times exhibited in the AS tasks (~450 ms longer than EO) result from both longer decision-making time (~300 ms) and longer non-decision time (~150 ms). However individual differences are apparent in both decision and non-decision time as shown in Figure 2, which we exploited to investigate the relationship between decision-making time and the readiness potential in the section titled "RP Duration as a Predictor of Response Time and Decision Time".

Comparison of Readiness Potentials between Action Selection and Execution Only Tasks

We calculated the response-locked evoked potentials for each subject to evaluate if the longer response times in the AS task compared to EO task were reflected in the readiness potential (RP). The readiness potential is a negative potential that begins prior to the response and reaches a negative peak at movement onset. Figure 3A shows the average across subjects of the RPs at the eight channels with the strongest negative potential, selected from all channels, for both tasks. In our experiment, the button push corresponds to the completion of shoulder internal or external rotation, so the minimum precedes the response marker by around 225 ms. This has little impact on the interpretation of the results, as the movement was identical in the two tasks and the RP reaches a minimum at the same time around -250 to -200 ms in each participant and task. Figure 3B shows the EEG topographies of the averaged potentials over the time period of the minimum peak (-250 ms to -200 ms). In these data the RP shows a strong negative potential close to the midline but slightly left-lateralized.

The duration of the readiness potential was defined as the time interval from the initial negative deflection of the readiness potential, i.e., when the signal shows a consistent negative ramp, to the button press indicating completion of movement. The duration of the RP for the AS task ($\bar{x}$ = 875 ms, s = 86 ms) was longer than the duration of RP for the EO task ($\bar{x}$ = 689 ms, s = 144 ms), a difference of almost 200 ms. RP duration was compared between tasks using a mixed-effects ANOVA with participants as a random factor. There was a significant difference in RP duration between the AS task and the EO task; $F(1,14) = 20.72$, $p < .0001$, with $BF = 501$ indicating substantial evidence to support a longer duration of the readiness potential in the AS task.

Comparison of Stimulus-locked EPs between Action Selection and Execution Only Tasks

We calculated stimulus-locked evoked potentials (EPs) for each subject in each task. Figure 4A shows the stimulus-locked evoked potentials at the eight channels that showed the strongest negative potential for the RP. Similar to the RP, the stimulus-locked EPs show a strong negative deflection at these electrodes. The onset of this negative potential occurred at a similar time for the AS task ($\bar{x}$ = 219 ms, s = 41 ms) and the EO task ($\bar{x}$ =248 ms, s = 19 ms). A mixed-effects ANOVA for the onset times of the negative deflection treating participants as a random factor showed no significant effect of task on onset times $F(1,14) = .35$, $p = .57$, with the Bayes Factor ($BF = 0.41$) indicating highly ambiguous evidence regarding the difference between means. The striking difference between tasks is the extended duration of the negative potential in the AS task as compared to the EO task. Both tasks show a negative potential that reaches a peak magnitude roughly 300 ms after stimulus onset. For the EO task this is the peak for all 8 channels while for the AS task 4 channels reach a minimum at 300 ms as in the EO task, but 4 of the channels reach a minimum 850 ms after stimulus onset. Figure 4B shows topographic maps of the potential at selected time points. For the AS task, the stimulus-locked EP at 300 ms post-stimulus is characterized by a strong positive potential over parietal channels, and a negative potential is strongest at electrodes anterior to the 8 channels with the strongest RP. This difference is topography in comparison to the RP indicated the stimulus-locked evoked potentials includes a different brain signal, specifically the P300 or the closely-related CPP (Philastides et al., 2006; Ratcliff et al., 2009; O'Connell et al., 2012; Kelly & O'Connell 2013). This observation is confirmed in Figure 4C which shows 8 channels over parietal cortex with a clearly visible P300. In contrast, 850 ms after the stimulus the topographic map indicates a strong negative potential with topographic distribution closely corresponding to the RP (see Figure 3B) and very little positive potential over parietal channels which have returned to baseline (Figure 4C). In Figure 4, the EO task shows a topographic distribution at 300 ms which incorporates both the negative potential at electrodes exhibiting the strongest RP and the positive potential over parietal cortex. The positive potential at parietal electrodes has smaller magnitude and shorter duration as shown in Figure 4C.

Evoked Potentials by Response Time Tertiles

We investigated if the readiness potential onset or duration was directly linked to the response times. For each subject, and in each task, the trials were sorted by response time and both stimulus and response-locked evoked potentials were separately averaged for the trials in the slowest, middle, and fastest RT tertiles, as shown in Figure 5.

For the AS task (Figure 5A), the fastest RT tertile had the shortest RP duration ($\bar{x}$ = 760 ms, s = 134 ms), then the middle RT tertile had longer RP duration ($\bar{x}$ = 815 ms, s = 105 ms) and the slowest RT tertile had the longest RP duration ($\bar{x}$ = 1081 ms, s = 143 ms). For the EO task, the fastest ($\bar{x}$ = 630 ms, s = 122) and middle ($\bar{x}$ = 606 ms, s= 182 ms) RT tertiles had similar RP duration while the slowest RT tertile ($\bar{x}$ = 949 ms, s = 125 ms) had about 300 ms longer RP duration. A mixed effects ANOVA was used to estimate the effect of task and RT tertile on RP onset times treating subjects as a random factor. There was no significant interaction between task and the tertile split; $F(2,14) = 1.32$, $p = .35$, with $BF = 0.3$. There was a significant effect of task; $F(1,28) = 25.69$, $p < .001$, with very strong evidence for a difference in mean onset time between tasks ($BF = 10^2$), and a significant effect of RT tertile; $F(2,28) = 59.79$, $p < .05$, with decisive evidence of a difference in mean onset time between RT tertiles ($BF = 10^{11}$).

In contrast, the stimulus-locked EP had onset times of the readiness potential (RP) that were similar for the three RT tertiles in both tasks as shown in Figure 5B. For the AS task, the fastest RT tertile had a RP onset at 201 ms (s = 50 ms), the middle RT tertile had a RP onset at 216 ms (s = 46 ms), and the slowest RT tertile had a RP onset at 224 ms (s = 44 ms). For the EO task, the fastest RT tertile had a RP onset of 206 ms (s = 101 ms), the middle RT tertile had a RP onset of 220 ms (s = 62 ms), and the slowest RT tertile had a RP onset of 221 ms (s = 71 ms). Relative to the stimulus presentation, the onset times of the RP did not account for differences in the response time tertiles. A mixed-effects ANOVA was used to estimate the effect of task and RT tertile on onset time treating subjects as a random factor. There was no significant effect found in tasks; $F(1,28) = .01$, $p = .94$, and substantial evidence for no effect of task ($BF = 0.6$) nor any effect for the three RT tertiles; $F(2,28) = .89$, $p = .42$, and substantial evidence for no effect of RT tertile (BF= 0.16).

RP Duration as a Predictor of Response Time and Decision-Making Time

We tested if the duration of the readiness potential (RP) was quantitatively related to response time and decision-making time. A linear regression analysis was performed to determine if RP duration could predict RT for each task, using the RP duration and median RT computed for each RT tertile in each subject. For the AS task, RP duration was strongly correlated to median

RT; $R^2 = .53$, $F(2,43) = 48.1$, $p < .01$, with decisive evidence of non-zero slope ($BF = 10^{13}$). RP duration had a nearly one-to-one relationship with RT for this task (Figure 6A) with $\beta = .94$ ($t(43) = 6.94$) and with some direct evidence of a regression slope of 1 ($BF1 = 19.25$). The intercept of 187 ms reflects additional time required to account for RT, possibly reflecting visual stimulus processing time, and is consistent with the roughly 200 ms onset time of the negative deflection in the stimulus-locked EP (Figure 5B).

Decision-making time (DT) was calculated for each trial by subtracting the non-decision time (median of the posterior distribution of non-decision time estimated by the drift-diffusion model) from the RT on each trial. Similar to the RT tertile analysis, the trials were sorted by DT and evoked potentials were estimated for three tertiles of DT to estimate RP duration. The RP durations for DT tertiles were combined across subjects to estimate a regression model. The relationship between RP duration and median DT was somewhat stronger; $R^2 = .59$, $F(2,43) = 62.3.$, $p < .01$, with $BF = 10^{16}$, and the RP duration also had a nearly one-to-one relationship to DT (Figure 6B) with $\beta = .92$ ($t(43) = 7.9$) and $BF1 = 7.21$. The intercept of -252 ms is consistent with the additional 250 ms for performance of the response, indicated by the time from the minimum of the RP to the response marker.

In contrast, for the EO task, the model did not perform as well for either RT and DT. There was a weaker (but significant) correlation between RP duration and RT; $R^2 = .29$, $F(2,43) = 17.1$, $p < .01$, with $BF = 10^5$ (Figure 6C) and a slope far less than one, $\beta = .36$, $t(43) = 4.14$ and $BF1 < 10^{-4}$. There was also a weaker (but significant) relationship between RP duration and DT; $R^2 = .34$, $F(2,43) = 20.4$, $p < .05$, with $BF = 10^6$. (Figure 6D) and a slope far less than one, $\beta = .34$, $t(43) = 4.52$ and $BF1 < 10^{-4}$.

Surface Laplacian analysis of the RP

The RPs in each subject were processed with a surface Laplacian to identify superficial focal current sources. In both tasks, with the application of a surface Laplacian, the current density estimates were localized over the midline somewhat anterior to bilateral motor cortex. Three electrodes were positioned over the strongest signals, and the time course shows that of these three, one electrode over the right midline area showed a positive signal while two electrodes over the left midline area showed a negative signal in both tasks (Figure 7A). This suggests that the RP involves a lateralization of current density in areas of the motor system that generate the RP. Figure 7B shows the topographies of the surface Laplacian averaged over -250 ms to -200 ms before the response, and the three electrodes with the highest magnitude current density are marked in green, red, and blue and labeled 1-3, corresponding to the waveforms in Figure 7A.

The overall pattern shows that the right hemisphere exhibited more positive current density in comparison to the left hemisphere, for both of these tasks involving right arm movement.

Discussion

Evidence accumulation is believed to be the underlying mechanism of decision-making, determining the time it takes to select between alternative decisions. Previous studies have shown parietal cortex activity that exhibits characteristics of evidence accumulation, and whose time is related to response time. In this study, an Action Selection task (O'Shea et al., 2007) was used to investigate decision-making. This task required participants to remember and apply an abstract rule to select one of two possible actions. Response time and accuracy data was fit to a drift-diffusion model (Ratcliff and McKoon, 2008) in order to partition response time into non-decision time (for perceptual processing and motor execution) and decision-making time. We found that the duration of the RP recorded over motor-related areas of the brain has a one-to-one relationship with decision-making time.

Readiness Potential reflects decision making in the Action Selection task

Our main objective in this study was to identify EEG signals whose timing shifted in a manner consistent with the longer decision-making time in the Action Selection (AS) task as compared to the Execution Only (EO) task. We expected that the variability in the RTs between the two tasks would be largely due to the abstract rule component of the AS task. Participants exhibited response times ~450 ms longer in the AS task than the EO task that was accounted for in the drift-diffusion model by both longer decision-making time (~280 ms) and longer non-decision time (~170 ms).

Readiness potentials (RPs) displayed the characteristic of slow ramping negativity reaching a minimum at the start of movement, resolving to baseline as the movement completed. The duration of the RPs (absolute value of the RP onset time) from the AS task was on average ~190 ms longer than the duration of the RP from the EO task. The stimulus-locked EPs at the same channels exhibited a negative ramp that onset identically at around 200 ms for both tasks indicating that the onset of the readiness potential takes place after visual encoding but before decision-making. Past work showed that variation in stimulus intensity did not effect RP duration (Miller et al, 1999), indicating that that RP is independent of perceptual processing. This suggests that the longer RPs in the AS task reflected longer decision-making time.

To clarify if RP quantitatively tracked decision-make time, a linear regression analysis was done with the tertile split of trials by response times (RTs) and decision-making times (DTs). In the AS task, RP duration and RT had a strong relationship with a slope close to 1 (.94), indicating

one-to-one relationship between increasing duration of readiness potential and response time (Figure 6A). The intercept in this model was 187 ms which was consistent with time for perceptual processing (Thorpe et al., 1996; Nunez et al., 2018), and with the onset of the readiness potential identified in the stimulus-locked EPs (~200 ms). RP duration and DT had a stronger regression model (Figure 6B) also with a slope close to 1 (.92), indicating a one-to-one relationship between RP duration and DT. In this model, the intercept of -252 ms accounted for the time from movement onset to complete the rotation, as is consistent with the timing of the negative peak of the readiness potential relative to the button push. These models provide strong evidence that RP duration tracks decision-making time, and that the intercepts of the two models account for the non-decision time of the drift diffusion model (stimulus processing and motor execution).

In the EO task, RP duration did not predict DT and RT as well as it did in the AS task. A lack of variability in the EO task RTs, compared to AS task RTs, may partially explain this finding, as shown in Figure 2. Moreover, in the EO task, the decision of which action to execute is fixed. As a consequence, variability in response time or decision-making time may be more strongly influenced by variability due to stimulus processing (detection) or response execution than in decision-making.

P300/CPP does not track decision-making in the Action Selection task

In previous studies, P300/CPP amplitude and timing of peak positive potential have been found to be reflective of evidence accumulation process towards a decision. In vigilance tasks (specifically gradual reduction in contrast & motion detection task with different coherence levels), the peak of CPP/P300 was delayed as RT increased (O'Connell et al., 2012; Kelly & O'Connell 2013). As the difficulty of identifying and processing the stimulus increased, there was a delay in the CPP/P300, with a peak right before motor execution. This was attributed to longer decision-making since the peak of the CPP/P300 occurred at motor execution. However, some of this delay may also reflect increased time for perceptual processing, as these studies employed stimuli at varying stimulus-to-noise ratios.

The task we have used in this study employed simple shapes presented without any noise, and the decision-making requires remembering and applying an abstract rule to decide on a response. The P300 was identified in each task, but the time of the peak was similar in the AS and EO tasks, despite the difference in response times (Figure 4C). Moreover, when the data were split into tertiles of fastest, middle, and slowest response times, the P300/CPP peaked at around the same time for the both tasks as reflected in the first negative peak of the stimulus-locked EP over motor areas in Figure 5B. It is possible that in the previous studies (O'Connell et al., 2012; Kelly

& O'Connell, 2013), the ambiguity of the stimulus lead to delayed stimulus detecting and encoding which contributed to a delayed CPP/P300.

Decision making includes both perceptual categorization and response selection. The CPP/P300 may reflect an evidence accumulation process for perceptual categorization. In the Action Selection (AS) task, perceptual categorization was not decisive in determining response time. Perceptual processing is simple, and the decision-making relies on information processing outside of perception. Our findings indicate that the readiness potential (RP) reflects evidence accumulation in the motor system for response selection, which is decisive in determining response time.

Evidence accumulators in the human brain

Reaction time (RT) and choice behavior during visual decision-making tasks are well characterized by models that assume a continuous stochastic accumulation of evidence (Link & Heath, 1975; Ratcliff & McKoon, 2008; Brown & Heathcote, 2008; Usher & McClelland, 2001; Ratcliff et al., 2016) Studies in animal models showing increasing firing rates in parietal cortex during perceptual decision-making (Roitman and Shadlen, 2002; Huk and Shadlen, 2005, Churchland et al., 2008), motivated the earlier studies of the P300 in parietal cortex (Philastides et al 2006; Ratcliff et al., 2009; O'Connell et al., 2012; Kelly & O'Connell 2013) and the present study of the readiness potential over motor-related areas of the brain. However, the relationship between progressively increasing firing rate and ramps in slow-wave EEG potentials are complicated by a number of factors. EEG potentials reflect synchronous synaptic potentials at a macroscopic (cm) scale (Nunez & Srinivasan, 2006). The sources of the EEG are the currents in extracellular space - EPSPs generate positive sources inside the membrane and negative current in the extracellular space while IPSPs generate negative sources inside the membrane and positive current in extracellular space. Thus, increasing firing rates might be expected to generate increased negative potentials as negative extracellular potentials reflect (locally) more EPSPs, suggesting that a negative ramp is related to increased cortical excitability facilitating firing of action potentials. However, we are cautious about this interpretation of the readiness potential (RP) because of the physics of EEG recording. Scalp potentials are recorded at a distance from the cortex, and thus dominated by dipole components of the brain current source distribution (Nunez & Srinivasan, 2006). Thus, the sign of the observed potential may merely reflect whether the negative or positive pole of the dipole is closer to the scalp. Despite this complication, it is reasonable to interpret a slow ramp in EEG potentials (of either sign) as a correlate of progressive change in firing rates, providing a means to investigate accumulator processes in the human brain.

Sources of the Readiness Potential

The scalp topographies of the RP reveal that the strongest negative potentials occur over motor areas close to the midline and anterior to C3/C4 (Figure 3B). The Bereitschaftspotential (BP) for finger movements is composed of an early shallow ramp over midline areas, such as supplementary motor areas (SMA) and pre-SMA and a steeper negative slope over contralateral motor areas (corresponding to C3/C4) that reaches a negative minimum at movement onset. In our task, which involved shoulder internal/external rotation movements, the RP had a focus entirely over midline areas from RP onset to movement onset, consistent with activity in the shoulder representation in primary motor cortex which is located close to the midline (Penfield & Rasmussen, 1950), The higher spatial resolution of the surface Laplacian (Figure 7) clearly indicated a focal source close to the midline, with opposite polarities between hemispheres.

Conclusion

Decision making has several underlying components including stimulus encoding, perceptual categorization, response selection, and response execution. In this study we made use of a task where stimulus identification is easy and response selection requires cognitive computations and working memory. In this scenario, we find that the duration of a signal linked to the motor system, the readiness potential, has a one-to-one relationship with amount of time required to make the decision, which is modeled by a stochastic evidence accumulation process. This close relationship between the readiness potential and the evidence accumulation process supports the notion that an accumulator process is a general neural implementation of decision-making in both sensory and motor systems, both when individuals take actions in response to stimuli (Shadlen and Kiani, 2013) or of their own free will (Schurger et al., 2012). Our results suggests that whether sensory or motor systems account for variability in decision making will depend on the location of the bottleneck in information processing.

Acknowledgements

This research was supported by a grant from the NSF to JV and RS (1658303) and grants from the NIH to SC (K24HD074722, T32AR047752, and K99HD091375) and from the University of California, Irvine Institute for Clinical and Translational Science to JC (UL1-TR000153).

References

Alexander, P., Schlegel, A., Sinnott-Armstrong, W., Roskies, A. L., Wheatley, T., & Tse, P. U. (2016). Readiness potentials driven by non-motoric processes. *Consciousness and Cognition,39*, 38-47. doi:10.1016/j.concog.2015.11.011

Brown, S. D. & Heathcote, A. (2008). The simplest complete model of choice response time: linear ballistic accumulation. *Cognitive Psychology*, 57(3), 153-178. doi: 10.1016/j.cogpsych.2007.12.002

Churchland, A. K., Kiani, R., & Shadlen, M. N. (2008). Decision-making with multiple alternatives. *Nature Neuroscience,11(6)*, 693-702. doi:10.1038/nn.2123

Deng S., Winter W., Thorpe S., Srinivasan R. (2012) Improved Surface Laplacian Estimates of Cortical Potential Using Realistic Models of Head Geometry. *IEEE Transactions on Biomedical Engineering* 59:2979-85.

Dickey, J. M., & Lientz, B. P. (1970). The weighted likelihood ratio, sharp hypotheses about chances, the order of a Markov chain. *The Annals of Mathematical Statistics*, *41*(1), 214-226.

Dirk, J., Kratzsch, G. K., Prindle, J. P., Kröhne, U., Goldhammer, F., & Schmiedek, F. (2017). Paper-Based Assessment of the Effects of Aging on Response Time: A Diffusion Model Analysis. *Journal of Intelligence,5*(2), 12. doi:10.3390/jintelligence5020012

Eimer, M. (1998). The lateralized readiness potential as an on-line measure of central response activation processes. *Behavior Research Methods, Instruments, & Computers,30*(1), 146-156. doi:10.3758/bf03209424

Huk, A. C., & Shadlen, M. N. (2005). Neural Activity in Macaque Parietal Cortex Reflects Temporal Integration of Visual Motion Signals during Perceptual Decision Making. *Journal of Neuroscience,25*(45), 10420-10436. doi:10.1523/jneurosci.4684-04.2005

Kass, R., & Raftery, A. (1995). Bayes Factors. *Journal of the American Statistical Association, 90*(430), 773-795. doi:10.2307/2291091

Kelly, S. P., & O'Connell, R. G. (2013). Internal and external influences on the rate of sensory evidence accumulation in the human brain. *The Journal of Neuroscience*, 33(50), 19434–41. doi:10.1523/JNEUROSCI.3355-13.2013

Kim, J., & Shadlen, M. N. (1999). Neural correlates of a decision in the dorsolateral prefrontal cortex of the macaque. *Nature Neuroscience, 2(2)*, 176-185. doi:10.1038/5739

Kornhuber, H. H., & Deecke, L. (1965). Hirnpotentialänderungen beim Menschen vor und nach Willkurbewegungen, dargestellt mit Magnetband-Speicherung und Ruckwartsanalyse. *Pflugers Archiv,284*, 1-17.

Lee, M. D. and Wagenmakers, E.-J. (2014). Bayesian cognitive modeling: A practical course. Cambridge University Press.

Link, S. and Heath, R. (1975). A sequential theory of psychological discrimination. *Psychometrika*, 40(1), 77-105. doi:10.1007/BF02291481

Mazziotta, J.C., Toga, A.W., Evans, A.C., Fox, P., Lancaster, J., (1995) A probabilistic atlas of the human brain: theory and rationale for its development. NeuroImage 2: 89–101

Miller, J., Ulrich, R., & Rinkenauer, G. (1999). Effects of stimulus intensity on the lateralized readiness potential. *Journal of Experimental Psychology: Human Perception and Performance,25*(5), 1454-1471. doi:10.1037//0096-1523.25.5.1454

Mulder, M., van Maanen, L., and Forstmann, B. (2014). Perceptual decision neurosciences a model-based review. *Neuroscience*, (277), 872–884. doi:10.1016/j.neuroscience.2014.07.031

Nunez, M. D., Gosai, A., Vandekerckhove, J., & Srinivasan, R. (2018). Visual encoding signals around 200 milliseconds track onset of evidence accumulation during human decision making. *bioRxiv*, 275727. doi: 10.1101/275727

Nunez, M. D., Nunez, P. L., & Srinivasan, R. (2016). Electroencephalography (EEG): neurophysics, experimental methods, and signal processing. In Ombao, H., Linquist, M., Thompson, W. & Aston, J. (Eds.) Handbook of Neuroimaging Data Analysis (pp. 175-197), Chapman & Hall/CRC. doi: 10.13140/rg.2.2.12706.63687

Nunez, M. D., Srinivasan, R., & Vandekerckhove, J. (2015). Individual differences in attention influence perceptual decision making. *Frontiers in Psychology,6*. doi:10.3389/fpsyg.2015.00018

Nunez, M. D., Vandekerckhove, J., & Srinivasan, R. (2017). How attention influences perceptual decision making: Single-trial EEG correlates of drift-diffusion model parameters. *Journal of Mathematical Psychology,76*, 117-130. doi:10.1016/j.jmp.2016.03.003

Nunez, P.L., & Srinivasan, R. (2006) *Electric Fields of the Brain: The Neurophysics of EEG, 2nd ed.*, Oxford UP, New York.

Oldfield, R.C. (1971) The assessment and analysis of handedness: The Edinburgh inventory. *Neuropsychologia*, 9(1):97-113.

O'Connell, R. G., Dockree, P. M., & Kelly, S. P. (2012). A supramodal accumulation-to-bound signal that determines perceptual decisions in humans. *Nature Neuroscience*, 15(12), 1729–1735. doi:10.1038/nn.3248

O'Shea, J., Johansen-Berg, H., Trief, D., Göbel, S., & Rushworth, M. F. (2007). Functionally Specific Reorganization in Human Premotor Cortex. *Neuron, 54*(3), 479-490.

Polich, J., Ellerson, P.C., Cohen, J. (1996) P300, stimulus intensity, modality, and probability. *International Journal of Psychophysiology*, 23:55-62.

Penfield, W. N., & Rasmussen, T. (1950). *The cerebral cortex of man*. Macmillan.

Philiastides, M. G., Ratcliff, R., & Sajda, P. (2006). Neural Representation of Task Difficulty and Decision Making during Perceptual Categorization: A Timing Diagram. *Journal of Neuroscience,26*(35), 8965-8975. doi:10.1523/jneurosci.1655-06.2006

Philiastides, M. G., Heekeren, H. R., & Sajda, P. (2014). Human scalp potentials reflect a mixture of decision-related signals during perceptual choices. *Journal of Neuroscience*, *34*(50), 16877-16889.

Plummer, M. (2003, March). JAGS: A program for analysis of Bayesian graphical models using Gibbs sampling. In *Proceedings of the 3rd international workshop on distributed statistical computing* (Vol. 124, p. 125).

Ratcliff, R. (1978). A theory of memory retrieval. *Psychological review*, *85*(2), 59.

Ratcliff, R., & Mckoon, G. (2008). The Diffusion Decision Model: Theory and Data for Two-Choice Decision Tasks. *Neural Computation,20*(4), 873-922. doi:10.1162/neco.2008.12-06-420

Ratcliff, R., Philastides, M.G., Sajda, P. (2009) Quality of evidence for perceptual decision making is indexed by trial-to-trial variability of the EEG. *Proceedings of the National Academy of the Sciences*, 106 (16):6539–6544.

Ratcliff, R., Smith, P.L., Brown, S.D., McKoon, G. (2016) Diffusion Decision Model: Current Issues and History. *Trends in Cognitive Sciences*, 20:260-281.

Roitman, J. D., & Shadlen, M. N. (2002). Response of neurons in the lateral intraparietal area during a combined visual discrimination reaction time task. *Journal of Neuroscience,22*(21), 9475-9489.

Rouder, J.N., Morey, R.D., Speckman, P.L., Province, J.M. (2012) Default Bayes factors for ANOVA designs. *Journal of Mathematical Psychology*, 56:356-374.

Schurger, A., Sitt, J. D., & Dehaene, S. (2012). An accumulator model for spontaneous neural activity prior to self-initiated movement. *Proceedings of the National Academy of Sciences,109*(42). doi:10.1073/pnas.1210467109

Shadlen, M., & Kiani, R. (2013). Decision Making as a Window on Cognition. *Neuron,80*(3), 791-806. doi:10.1016/j.neuron.2013.10.047

Shibasaki, H., & Hallett, M. (2006). What is the Bereitschaftspotential? *Clinical Neurophysiology,117*(11), 2341-2356. doi:https://doi.org/10.1016/j.clinph.2006.04.025

Smith, P. L., & Ratcliff, R. (2004). Psychology and neurobiology of simple decisions. *Trends in Neurosciences,27*(3), 161-168. doi:10.1016/j.tins.2004.01.006

Thorpe, S., Fize, D., & Marlot, C. (1996). Speed of processing in the human visual system. *Nature,381*(6582), 520-522. doi:10.1038/381520a0

Turner, B. M., van Maanen, L., & Forstmann, B. U. (2015). Informing cognitive abstractions through neuroimaging: The neural drift diffusion model. *Psychological Review*, 122(2), 312–336. doi:10.1037/a0038894

Turner, B. M., Forstmann, B. U., Love, B. C., Palmeri, T. J., & Van Maanen, L. (2017). Approaches to analysis in model-based cognitive neuroscience. *Journal of Mathematical Psychology*, *76*, 65-79. doi:10.1016/j.jmp.2016.01.001

Usher, M., & Mcclelland, J. L. (2001). The time course of perceptual choice: The leaky, competing accumulator model. *Psychological Review,108*(3), 550-592. doi:10.1037//0033-295x.108.3.550

Vandekerckhove, J., Tuerlinckx, F., & Lee, M. D. (2011). Hierarchical diffusion models for two-choice response times. *Psychological Methods*, 16, 44-62.

Wabersich, D., & Vandekerckhove, J. (2014). Extending JAGS: A tutorial on adding custom distributions to JAGS (with a diffusion model example). Behavior Research Methods, 46, 15-28

Wagenmakers, E. J., Lodewyckx, T., Kuriyal, H., & Grasman, R. (2010). Bayesian hypothesis testing for psychologists: A tutorial on the Savage–Dickey method. *Cognitive psychology*, *60*(3), 158-189.

Figures

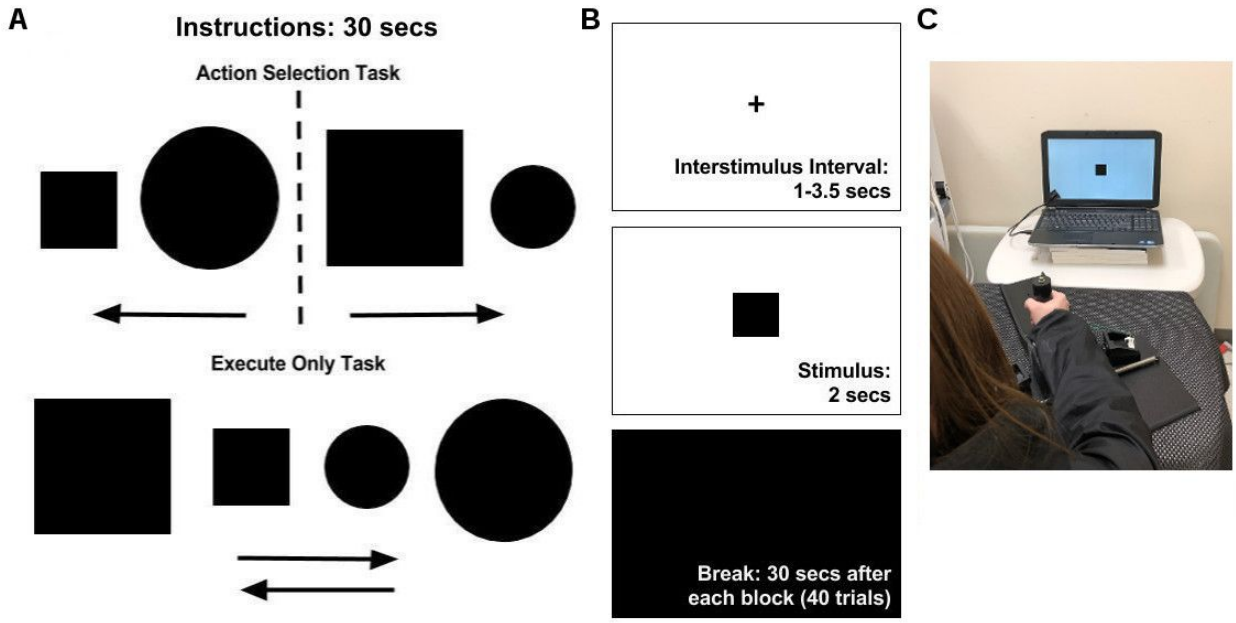

Figure 1: A. Participants received instructions prior to each block of 40 trials. The Action Selection (AS) task instructions directed the subjects to make an external rotation movement when a large square or small circle appeared, and an internal rotation movement when a large circle or small square appeared. For each Execution Only (EO) block, instructions directed participants to perform either an external rotation movement or an internal rotation irrespective of the stimulus. B. The time course of each trial. The participants fixated on a cross during an interstimulus interval of random duration ranging from 1 to 3.5 secs. A single stimulus was presented for two seconds during which responses were collected. After each block of 40 trials, participants received a 30 second break. C. The subjects used the lower arm splint apparatus to

make an internal (left) or external (right) rotation of 17.5 degrees to press a switch that captured their response. The splint was used to minimize any forearm or hand movements.

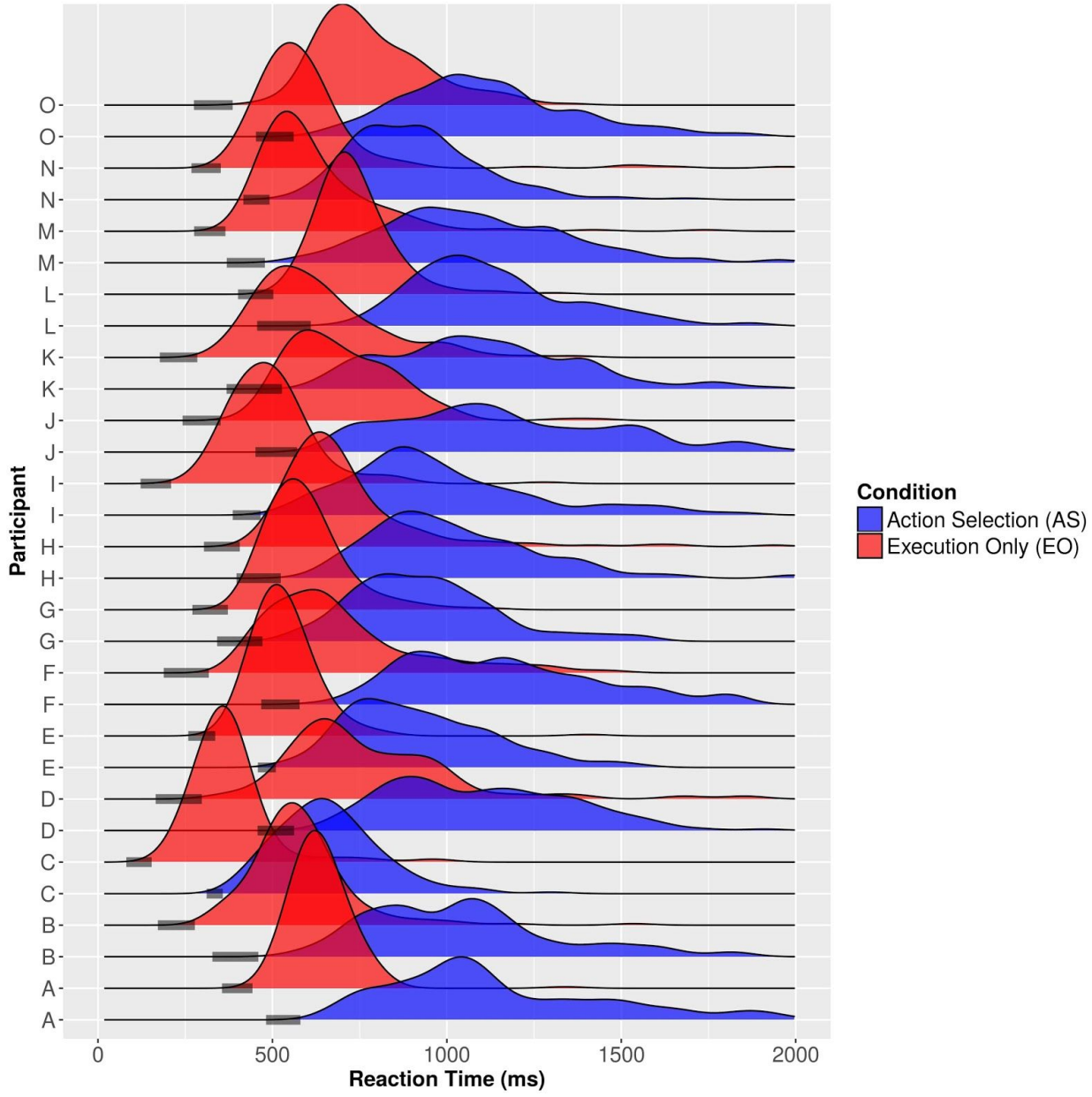

Figure 2: Response time distributions and estimated non-decision times for each participant. Each participant had a distribution of response times for both the AS and EO tasks. 95% credible intervals of non-decision time are given by the shaded bars on the response time axis.

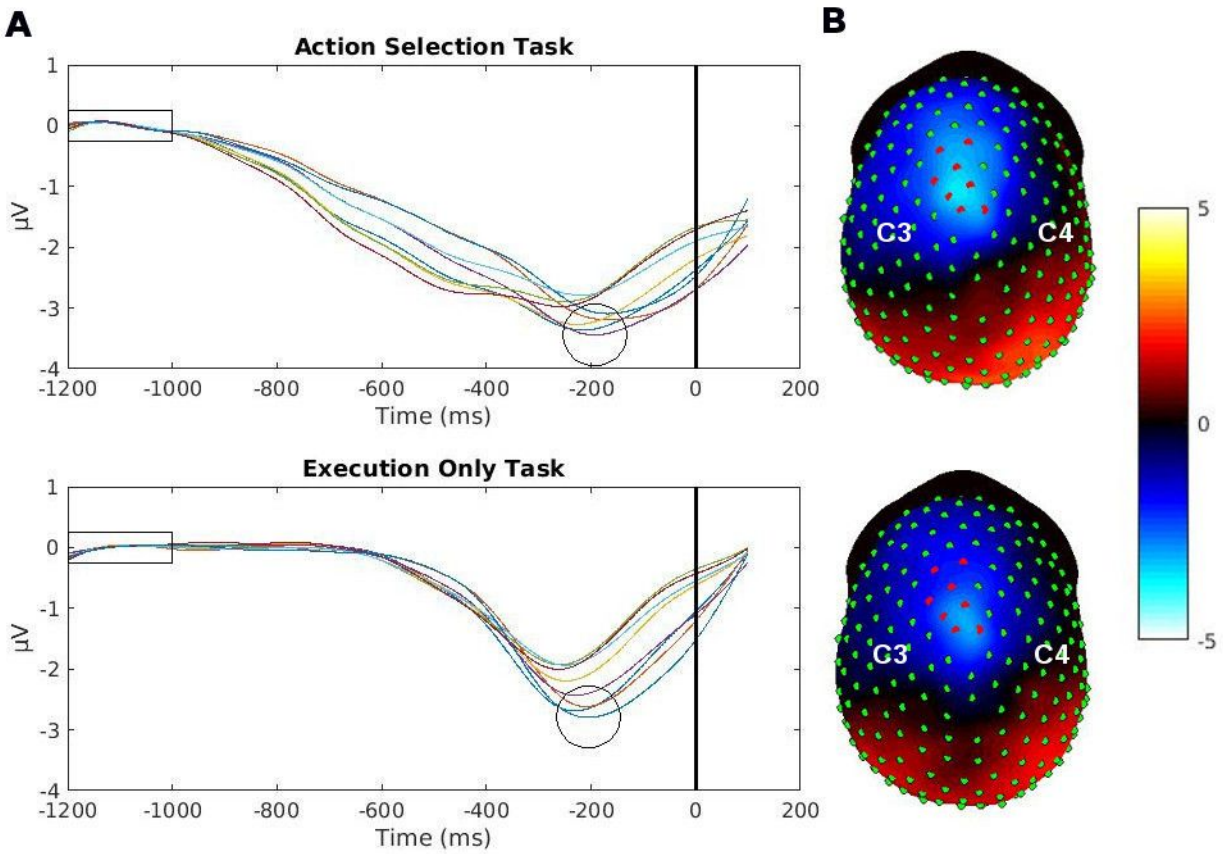

Figure 3: A) The response-locked (0 ms on the graph) RPs at the eight channels (red dots denoted in 3B) that showed the strongest negative potential for the two tasks. Each channel was averaged across the 15 participants. The circles indicate the minimum amplitude peak, which occurred around -200 ms for the both tasks. The common baseline is indicated by the rectangle, from -1200ms to -1000ms. In the AS task, the RP slowly ramps down to the negative minimum, compared to the EO task where the RP sharply ramps down to the minimum. B) The EEG topographies represent mean potentials of the time interval from -250 ms to -200 ms, where the minimum peak amplitudes occurred for the two tasks. The eight channels with the greatest negative potential, selected from all channels, are indicated in red and are located close to the midline over motor areas of the brain. The locations of the C3 and C4 channels over hand areas of the motor cortex are also indicated. The colorbar indicates $\mu Volts$.

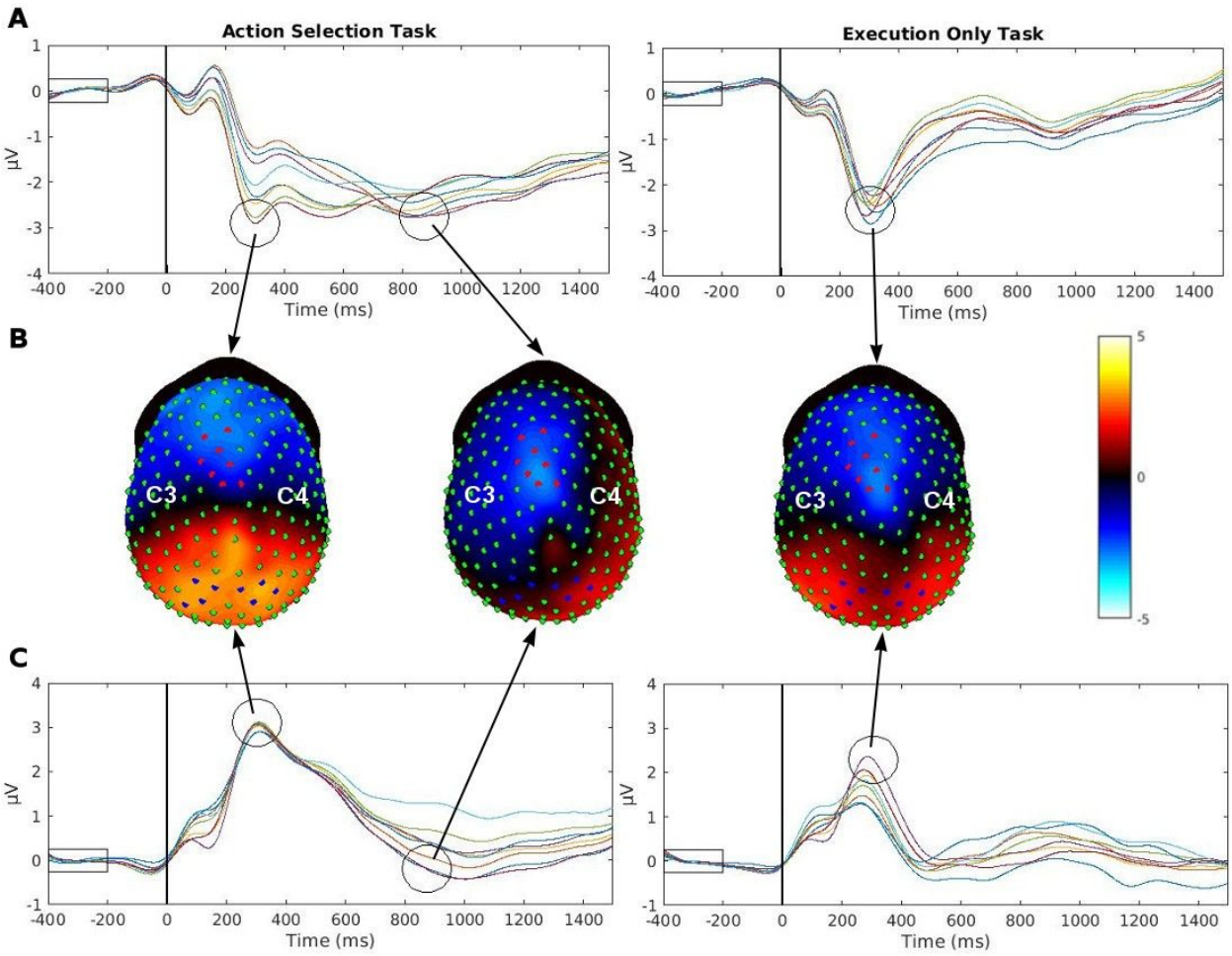

Figure 4: A) The time series of the the stimulus-locked EPs at the 8 channels that displayed the strongest negative RP, indicated by the red dots. The baseline, indicated by the rectangle, was set at -400ms to -200ms before the stimulus onset. In the AS task, 4 channels reached a negative peak at 300 ms while the other 4 channels reached a negative peak at 850 ms. In the EO task, all the channels reached a negative peak at 300 ms. B) In the AS task, the scalp topography is shown for the average potentials between 300ms to 350 ms revealing stronger negativity anterior to the 8 electrodes that showed the strongest RP (see Figure 3), and a strong positive potential over parietal cortex. The second negative minimum, which was averaged from 850ms to 900 ms, had strong negativity over the left midline area, similar to the RP distribution shown in Figure 3B, while the positive potential has diminished over the parietal areas. The negative peak in the EO task at 300 ms to 350 ms displayed a similar pattern with stronger negativity over the left midline area. The channels that displayed the strongest negativity in the RP are marked in red and the channels that displayed the strongest stimulus-locked positivity are marked in blue. The locations of C3 and C4 over motor cortex are indicated. C) The time series of 8 channels over the parietal cortex that showed the strongest positivity during the first negative minimum in the AS task. At the point of the second negative minimum, these channels are close to baseline. In the EO task,

there is a positive peak at parietal channels that occurs the same time as the negative peak for the left motor channels.

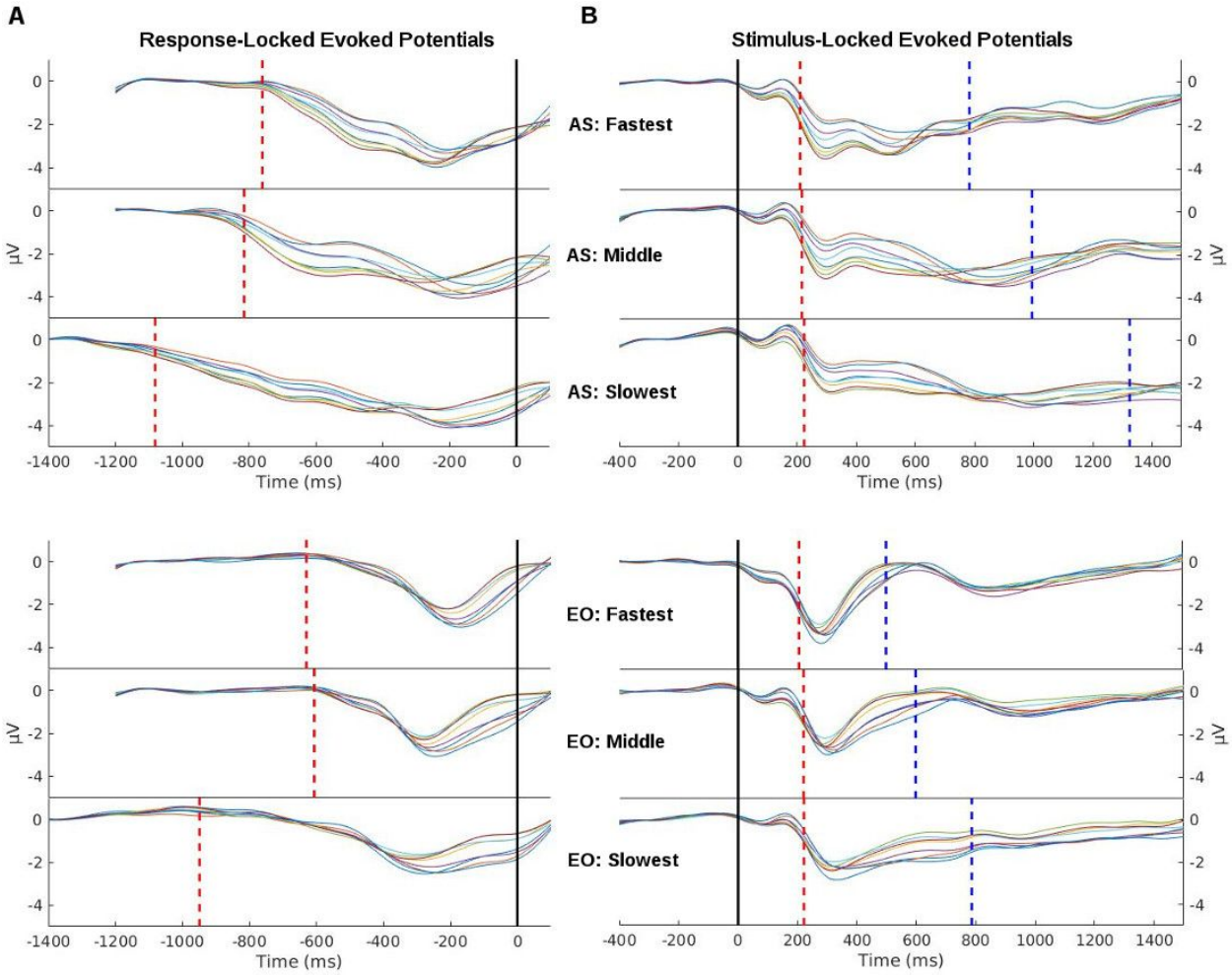

Figure 5: The evoked potentials of the 8 left motor cortex channels split into RT tertiles of fastest, middle, and slowest. A) The response-locked EPs for the fastest and middle tertiles are shown for a window of -1200 ms to 100 ms around the response indicated by a black vertical line. For the slowest RT tertile a longer window, -1400 ms to 100 ms around response, was used to accurately estimate RP duration. The red dotted lines represent the average RP duration in both tasks. In the AS task, the RP duration varied between conditions revealing the pattern of longer RTs had longer RP duration. For the EO task, the fastest and middle condition had similar RP durations, and the slowest had a 300 ms difference. B) The stimulus-locked EPs are shown with a window of -400 ms to 1500 ms around stimulus onset indicated by the black vertical line. The RP onset times were similar in both tasks for all tertiles as shown by the red dotted line. The blue dotted line represent the average RTs. *One subject was excluded from this figure because of very fast RTs compared to the other subjects. RP duration and onset times were estimated from*

this subject and included in the estimates of average duration and onset time and in the regression models shown in Figure 6.

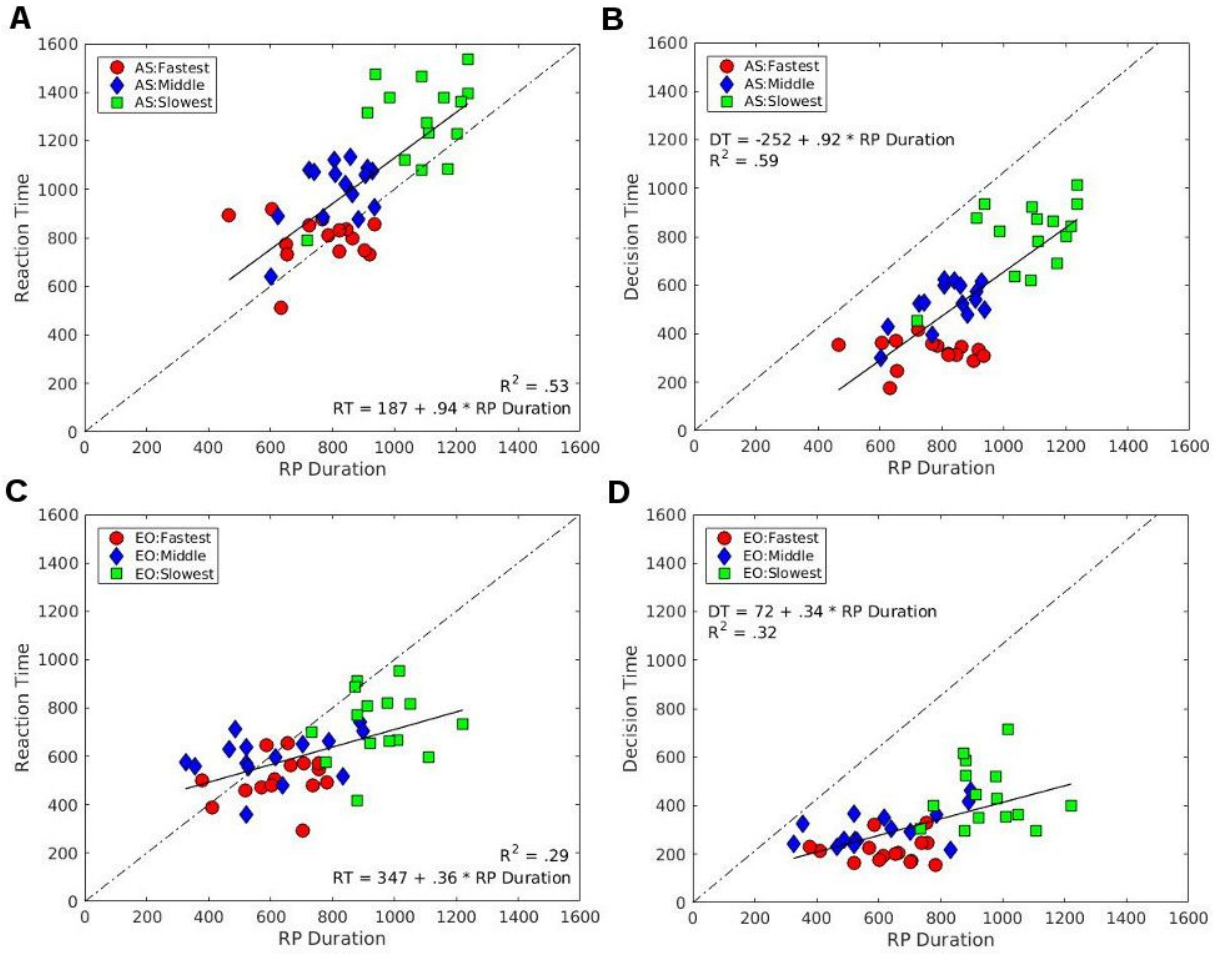

Figure 6: A) Regression model between RP duration (absolute value of RP onset time) and median response time for the AS task. B) Regression model between RP duration (absolute value of RP onset time) and median Decision Time for the AS task. C) Regression model between RP duration (absolute value of RP onset time) and median Response Time for For the EO task. B. Regression model between RP duration (absolute value of RP onset time) and Decision Time for the EO task. For the AS task, RP duration was strongly correlated to both RT and DT, with nearly a one-to-one relationship, indicating that the duration of RP was tracking decision-making process. For the EO task, the correlation was much weaker, and the slope less than one.

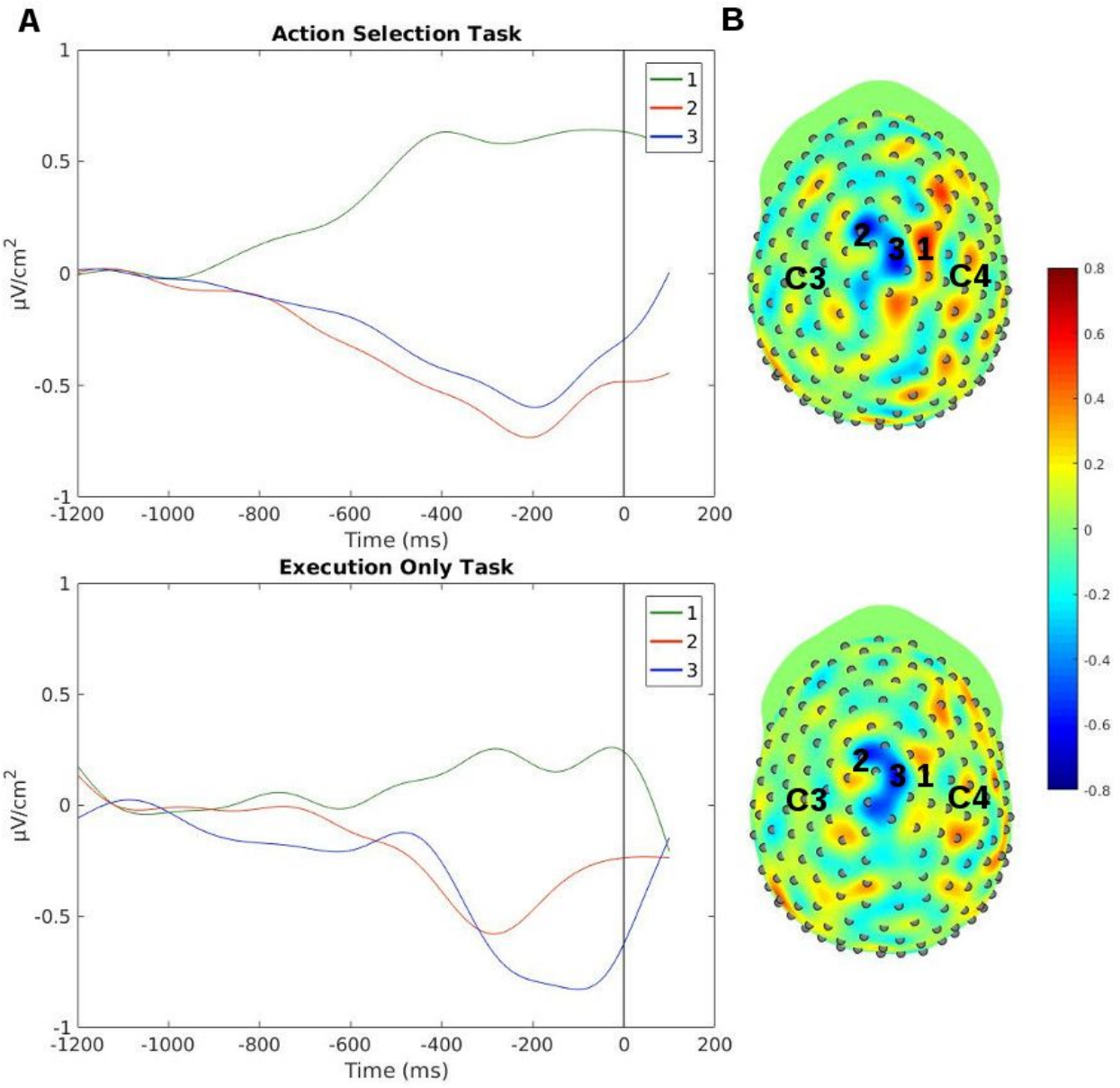

Figure 7: By applying a surface Laplacian, the strongest current density was localized close to the midline, potentially generated by bilateral structures in the motor cortex close to the midline. There were two electrodes that showed strong negativity over the left midline area and one electrode that showed strong positivity over the right midline area that could be suggestive of lateralization of the motor system. A) The time course of the 3 electrodes that generated the strongest current source density. B) The topography of current source density with the surface Laplacian applied. The three midline electrodes with greatest activity are marked in red, green, and blue and labeled 1-3. For reference, C3 and C4 electrodes are labeled.